B4GALNT1 promotes hepatocellular carcinoma stemness and progression via integrin α2β1-mediated FAK and AKT activation

Authors

Yao Tang, Zhijie Xu, Fuyuan Xu, Juan Ye, Jianxu Chen, Jianzhong He, Yingchun Chen, Chunhui Qi, Hongbin Huang, Ruiyang Liu, Hong Shan, Fei Xiao

Correspondence

shanhong@mail.sysu.edu.cn (H. Shan), xiaof35@sysu.edu.cn (F. Xiao).

Graphical abstract

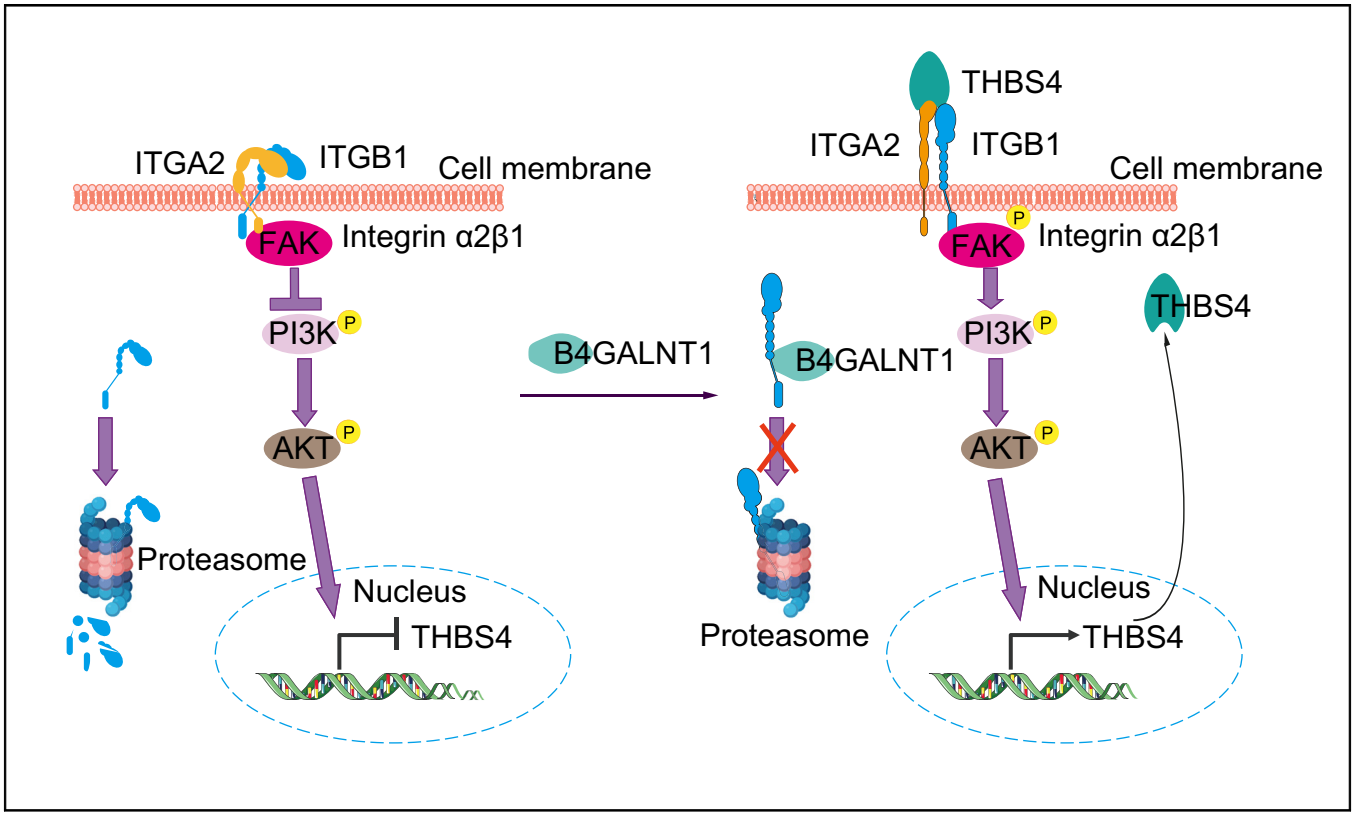

Highlights

- B4GALNT1 promotes HCC stemness, proliferation, invasion, migration, EMT and growth.
- Elevated B4GALNT1 predicts poor prognosis in patients with HCC.
- B4GALNT1 promotes HCC stemness and progression by regulating the integrin α2β1/FAK/PI3K/AKT axis.
- Ophiopogonin D could be a potential therapeutic drug for patients with HCC.

Impact and implications

The role and regulatory mechanism of B4GALNT1 in HCC have not been studied previously. Here, we reveal that B4GALNT1 has a crucial role in HCC stemness and progression by activating the integrin α2β1/FAK/PI3K/AKT axis, providing a potential target for HCC therapy. In addition, we find Ophiopogonin D as a potential therapeutic drug for patients with HCC.

https://doi.org/10.1016/j.jhepr.2023.100903

Research article

JHEP|Reports

B4GALNT1 promotes hepatocellular carcinoma stemness and progression via integrin α2β1-mediated FAK and AKT activation

Yao Tang,[1,2,†] **Zhijie Xu**,[1,2,†] **Fuyuan Xu**,[1,2,†] Juan Ye,[1,2] Jianxu Chen,[1,2] Jianzhong He,[4] Yingchun Chen,[1] Chunhui Qi,[1,2] Hongbin Huang,[1,2] Ruiyang Liu,[1,2] Hong Shan,[1,3,*] Fei Xiao[1,2,5,*]

[1]*Guangdong Provincial Engineering Research Center of Molecular Imaging, the Fifth Affiliated Hospital, Sun Yat-sen University, Zhuhai 519000, Guangdong, China;* [2]*Department of Infectious Diseases, the Fifth Affiliated Hospital, Sun Yat-sen University, Zhuhai 519000, Guangdong, China;* [3]*Center for Interventional Medicine, the Fifth Affiliated Hospital, Sun Yat-sen University, Zhuhai 519000, Guangdong, China;* [4]*Department of Pathology, the Fifth Affiliated Hospital, Sun Yat-sen University, Zhuhai 519000, Guangdong, China;* [5]*Kashi Guangdong Institute of Science and Technology, the First People's Hospital of Kashi, Kashi 844000, Xinjiang, China*

JHEP Reports **2023.** https://doi.org/10.1016/j.jhepr.2023.100903

Background & Aims: β-1,4-*N*-Acetyl-galactosaminyltransferase 1 (B4GALNT1) has been reported to contribute to the development of human malignancies. However, its role in hepatocellular carcinoma (HCC) remains uncharacterised. In this study, we aimed to elucidate the role of B4GALNT1 in HCC stemness and progression.

Methods: Immunohistochemical staining was used to evaluate B4GALNT1 expression in HCC tissues and adjacent normal liver tissues. Flow cytometry analysis and sphere formation analysis were performed to investigate the role of B4GALNT1 in HCC stemness. Colony formation, Incucyte, wound-healing, Transwell migration, and invasion assays, and an animal model were used to study the role of B4GALNT1 in HCC progression. RNA-sequencing and co-immunoprecipitation were used to investigate the downstream targets of B4GALNT1.

Results: B4GALNT1 was upregulated in HCC and associated with poor clinical outcome of patients with the disease. Moreover, B4GALNT1 promoted HCC stemness, migration, invasion, and growth. Mechanistically, B4GALNT1 not only promoted the expression of the integrin α2β1 ligand THBS4, but also directly interacted with the β subunit of integrin α2β1 ITGB1 to inhibit its ubiquitin-independent proteasomal degradation, resulting in activation of FAK and AKT. Ophiopogonin D inhibited HCC stemness and progression by reducing ITGB1 and THBS4 expression and inhibiting FAK and AKT activation.

Conclusions: Our study suggests the B4GALNT1/integrin α2β1/FAK/PI3K/AKT axis as a therapeutic target for the inhibition of HCC stemness and tumour progression.

Impact and implications: The role and regulatory mechanism of B4GALNT1 in HCC have not been studied previously. Here, we reveal that B4GALNT1 has a crucial role in HCC stemness and progression by activating the integrin α2β1/FAK/PI3K/AKT axis, providing a potential target for HCC therapy. In addition, we find Ophiopogonin D as a potential therapeutic drug for patients with HCC.

Introduction

Primary liver cancer is the seventh most common cancer and was the third leading cause of cancer-related mortality worldwide in 2020.[1] As the dominant histological type of liver cancer, hepatocellular carcinoma (HCC) accounts for the majority of liver cancer incidence and mortality rates.[2] Despite the availability of a comprehensive regimen including liver transplantation and resection, ablation, chemoembolisation, and systemic therapies, such as immune-checkpoint inhibitors, tyrosine kinase inhibitors, and monoclonal antibodies, the outcome for patients with advanced HCC remains poor.[3] Therefore, a better understanding of the key regulators that promote HCC initiation and progression will facilitate the development of novel therapeutic strategies.

β-1,4-*N*-Acetyl-galactosaminyltransferase 1 (B4GALNT1) is a crucial enzyme is involved in the synthesis of gangliosides, such as GM2 and GD2, both of which are important cancer antigens that are highly expressed in several tumour types.[4] The involvement of B4GALNT1 in multiple types of tumour has been reported in recent years. For example, B4GALNT1 promotes melanoma angiogenesis and growth by inducing GM2/GD2.[4] It also promotes lung adenocarcinoma metastasis by activating the JNK/c-Jun/Slug pathway.[5] In addition, B4GALNT1 can regulate clear cell renal cell carcinoma metastasis through the focal adhesion and Hippo signalling pathways.[6] However, the role and regulatory mechanism of B4GALNT1 in HCC have not yet been reported.

Integrins are a family of heterodimeric cellular adhesion receptors comprising α- and β-subunits and regulate cell–cell and

Keywords: B4GALNT1; ITGB1; THBS4; Hepatocellular carcinoma.
Received 4 January 2023; received in revised form 17 August 2023; accepted 22 August 2023; available online 5 September 2023

† These authors contributed equally to this work.

* Corresponding authors. Address: Guangdong Provincial Engineering Research Center of Molecular Imaging, the Fifth Affiliated Hospital, Sun Yat-sen University, 52 Mei Hua East Road, Zhuhai 51900, Guangdong Province, China. Tel./fax: +86 765 2528527. (H. Shan) (F. Xiao).
E-mail addresses: shanhong@mail.sysu.edu.cn (H. Shan), xiaof35@sysu.edu.cn (F. Xiao).

cell–extracellular matrix (ECM) interactions. The conformational changes of integrins induced by integrin–ligand interactions recruit several cytoplasmic proteins to form a large protein complex, which further recruits and activates various protein kinases to activate the FAK/PI3K/AKT or RAS/MAPK pathway.[7,8] Integrins have been demonstrated to regulate HCC initiation and progression. For instance, integrin α2β1, which comprises integrin α2 (ITGA2) and integrin β1 (ITGB1), promotes the growth and TGFβ1-, bFGF-, and EGF-stimulated metastasis of HCC.[9,10] However, the mechanisms that regulate integrin α2β1 activation remain largely unknown.

CRISPR screening is a powerful tool for forward genetic screening to identify key regulators of tumour initiation and progression.[11] Liver cancer stem cells (LCSCs) are a subpopulation of HCC cells that are characterised by strong tumour-initiating abilities and have important roles in the initiation, maintenance, relapse, metastasis, and therapeutic resistance of HCC.[12] We previously performed a genome-wide CRISPR/Cas9 knockout screen and identified B4GALNT1 as one of the key factors that regulates HCC stemness. Here, we further investigated the role and regulatory mechanism of B4GALNT1 in HCC initiation and progression. We found that B4GALNT1 promoted HCC stemness, migration, invasion, epithelial–mesenchymal transition (EMT), and tumourigenicity by increasing THBS4 expression and ITGB1 stability to stabilise integrin α2β1–ligand complexes, leading to the activation of the FAK/PI3K/AKT pathway. In addition, we found that Ophiopogonin D (OP-D) could target B4GALNT1/integrin α2β1/FAK/PI3K/AKT signalling and, thus, propose it as a candidate drug for the treatment of HCC.

Materials and methods

Clinical tissues

Ninety-eight pairs of paraffin-embedded HCC tissues and corresponding adjacent normal liver tissues (ANTs) were obtained from the Fifth Affiliated Hospital of Sun Yat-Sen University, Zhuhai, China between January 2002 and December 2016. The diagnosis of HCC was confirmed by pathologists. Written informed consent was obtained from each patient. The study was based on the Declaration of Helsinki and approved by the medical ethics committee of the Fifth Affiliated Hospital of Sun Yat-Sen University (No. 2022-K105-1). Tissues from patients who had received chemotherapy or interventional treatments before surgical resection were excluded.

Cell culture

HCC cell lines PLC/PRF/5 (PLC), Huh-7, Hep3B, HepG2, and SNU-387, as well as immortal hepatocyte MIHA, were all purchased from the Cell Bank of the Chinese Academy of Sciences (Shanghai, China). PLC, Huh-7, Hep3B, and HepG2 cells were cultured in DMEM medium (Hyclone, USA) supplemented with 10% FBS (WISENT), penicillin G (100 U/ml), and streptomycin (100 mg/ml). SNU-387 and MIHA cells were cultured in RPMI1640 medium (GIBCO, USA) supplemented with 10% FBS, penicillin G (100 U/ml), and streptomycin (100 mg/ml). All cell lines were maintained at 37 °C with 5% CO_2.

RNA interference

To knockdown the expression of endogenous B4GALNT1 and ITGB1, the short hairpin (sh)RNA sequences against B4GALNT1 and ITGB1 were cloned into the PLKO.1-Puro vector. The Scramble control was used as the negative control. The sequences are shown in Table S1.

RNA isolation and quantitative real-time PCR

RNAzol®RT (MRC) was used to extract total RNAs from cells according to the manufacturer's protocol. cDNA was synthesised by using the HiScript III RT SuperMix kit (Vazyme, China). Quantitative real-time PCR (qRT-PCR) was performed using TB Green Premix Ex Taq II (TaKaRa, Japan). β-actin was used as an internal control and the relative expression of genes was calculated using the $2^{-\Delta\Delta Ct}$ method. The primers used for qRT-PCR are listed in Table S2.

Western blot

Cell lysates were extracted using RIPA lysis buffer (Beyotime Biotechnology, China). Protein concentration was determined by BCA assay (Thermo Fisher Scientific, USA). The proteins were separated using 10% SDS-PAGE gels and transferred onto PVDF membranes. The membrane was blocked with 3% bovine serum albumin (BSA) in PBS for 1 h at room temperature and then incubated with primary antibody overnight at 4 °C. The specific antibody dilution concentrations are detailed in Table S3. The membranes were washed with TBST and incubated with secondary antibodies for 1 h at room temperature. Finally, protein signals were detected using chemiluminescent HRP substrate (Millipore, USA).

Flow cytometry analysis

Cells were dissociated into single cells and counted. Then, 1×10^6 cells were resuspended in 100 μl 2% FBS and stained with APC-conjugated anti-CD133 (Miltenyi Biotec) and PE-conjugated anti-CD24 (BD Biosciences) antibodies on ice for 30 min in the dark. Cells were then washed once and resuspended in staining buffer [0.5 μg/ml DAPI (Sigma) in 2% FBS]. Samples were analyzed on CytoFLEX LX (Beckman) and data analysis was performed using FlowJo software.

Sphere formation

Next, 1×10^3 HCC cells were seeded into each well of 6-well ultra-low attachment plates and cultured in DMEM/F12 (GIBCO) supplemented with 1% B27 (STEMCELL Technologies, USA), 1% N2 (STEMCELL Technologies), 20 ng/ml EGF (Novoprotein, China), and 20 mg/ml bFGF (Novoprotein) for 2 wk.

Colony formation assay

HCC cells were seeded into 6-well plates with 500 cells/well and cultured for 2 wk. When there were at least 50 cells for a single clone, the clones were fixed, stained with 1% Crystal Violet, and counted.

Cell viability assay (Incucyte assay)

HCC cells were seeded at a density of $4–4.5 \times 10^3$ cells per well in 96-well plates. The confluence of the cells was assessed by the Incucyte Live-Cell Analysis System (LUMEX, China) for 100 h continuously after plating. All experiments were performed in 5 replicates per trial.

Wound-healing assay

HCC cells were cultured in 6-well plates until 90% confluence and then scratched with a 10-μl pipette tip. The wound width was observed and captured under the microscope at 0 h and 24 h after scratching.

Transwell migration and invasion assays

Transwell chambers (pore size 8 μm; Corning, USA) were used for migration (without Matrigel) and invasion (with Matrigel) assays. Briefly, 200 μl of cells (8–20 × 10^4 cells) resuspended in serum-free medium was layered in the upper chamber and medium containing 10% FBS was applied to the lower chamber. After incubating for 24 h, the cells of the upper chamber were discarded, and the cells of the lower chamber were fixed with 4% paraformaldehyde and stained with 0.1% Crystal Violet. Cells were counted in 5 random fields under the microscope.

Immunohistochemical staining

Paraffin-embedded tissues were cut into 4 μm-thick slices. After dewaxing and hydration, the slices were soaked in 3% hydrogen peroxide solution for 20 min at room temperature to block endogenous peroxidase. To retrieve antigen, the slices were heated at 95 °C in EDTA solution. The tissues were then incubated with goat serum for 1 h at room temperature followed by incubation overnight with primary antibodies. The specific antibody dilution concentrations are shown in Table S3. The slices were washed in PBS and incubated with secondary antibodies for 1 h at room temperature. Subsequently, the slices were stained with 3,3′-diaminobenzidine (DAB; Zhongshan Biotech, China) and counterstained with H&E. Finally, the slices were dehydrated and sealed. Two experienced pathologists independently evaluated the concentration intensity and percentage of the positive-staining cells. The values for B4GALNT1, THBS4, and ITGB1 staining intensity were assigned as follows: 0 (negative); 1 (weak); 2 (moderate); and 3 (strong). The values for the percentage of positive cells were scored as follows: 0 (0–5%); 1 (6–25%); 2 (26–50%); 3 (51–75%); and 4 (76–100%). The scores of the 2 aspects were multiplied together as the immunoreactive score for each slice.

Immunofluorescence

HCC cells were seeded in 24-well plates or 3.5-mm confocal dishes. After cell adherence, cells were fixed with 4% paraformaldehyde for 30 min and then blocked and permeabilised with PBS supplemented with 3% BSA and 0.2% Triton X-100 for 2 h at room temperature. Cells were then incubated with primary antibodies overnight at 4 °C. The specific antibody dilution

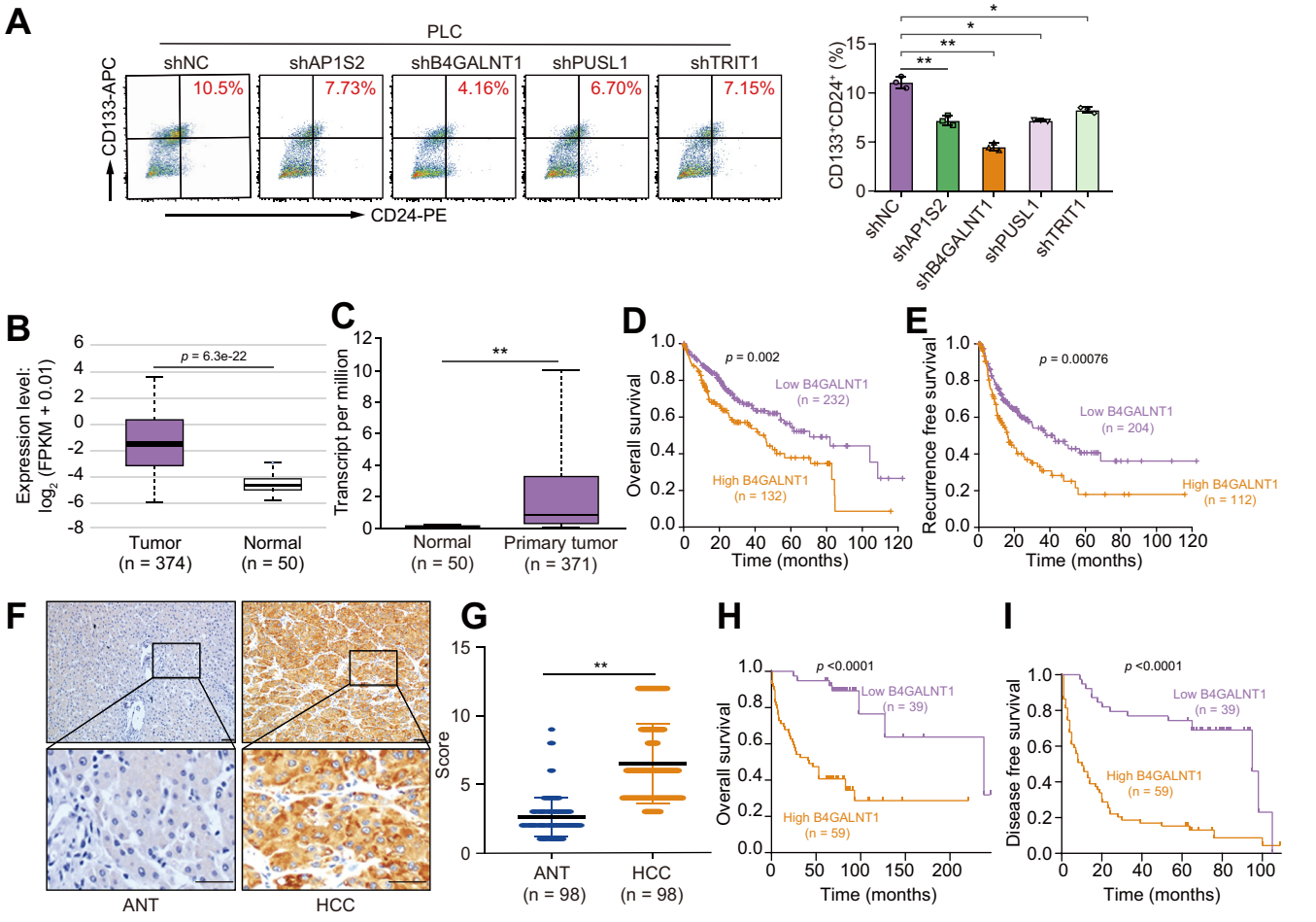

Fig. 1. B4GALNT1 is upregulated in HCC cells and tissues and positively correlated with poor clinical outcome. (A) Flow cytometry analysis of the effect of AP1S2, B4GALNT1, PUSL1, and TRIT1 knockdown on the percentage of $CD24^+CD133^+$ LCSCs in PLC cells. The mRNA level of *B4GALNT1* in HCC tissues and normal liver tissues in TCGA determined using StarBase v3.0 (B) and UALCAN (C). Kaplan-Meier curves for (D) overall survival and (E) recurrence-free survival of patients with HCC with high or low *B4GALNT1* expression. (F) Representative image of IHC staining of B4GALNT1 in HCC tissues and corresponding ANTs. (G) Protein level of B4GALNT1 in HCC tissues and paired normal liver tissues. Kaplan-Meier curves for (H) overall survival and (I) disease-free survival of 98 patients with HCC with low *vs.* high ITGB1 expression. Data are mean ± SEM for three technical replicates, analysed with Student's two-tailed *t* test; **p* <0.05, ***p* <0.01. Scale bars: 50 μm. ANT, adjacent normal liver tissue; B4GALNT1, β-1,4-*N*-acetyl-galactosaminyltransferase 1; HCC, hepatocellular carcinoma; IHC, immunohistochemistry; LCSC, liver cancer stem cell; PLC, PLC/PRF/5 cell line; shNC, negative control vector containing scrambled shRNA; TCGA, The Cancer Genome Atlas.

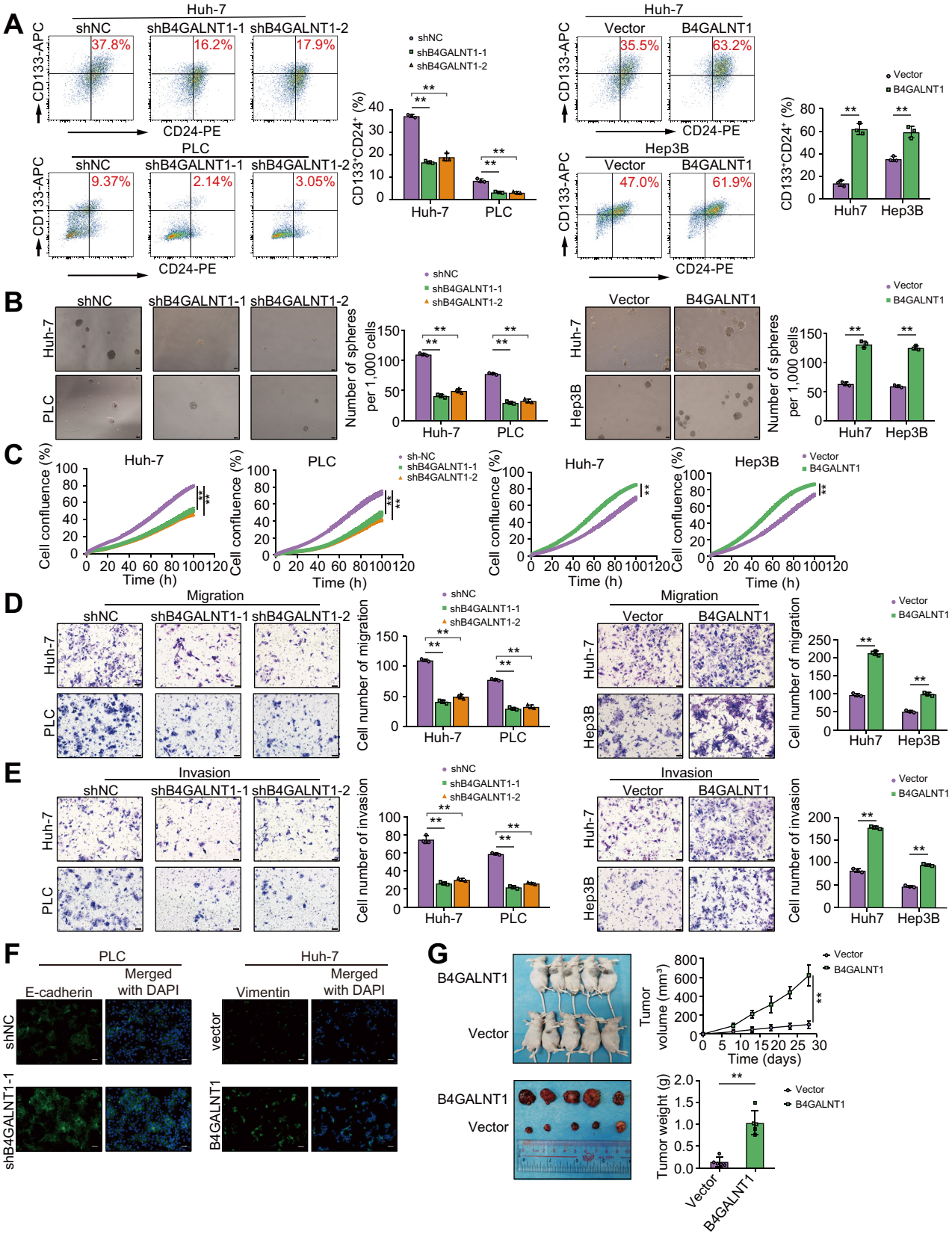

Fig. 2. B4GALNT1 promotes HCC stemness, proliferation, migration, invasion, and growth. (A) Flow cytometry analysis of the effect of B4GALNT1 knockdown or overexpression on the percentage of $CD24^{+}CD133^{+}$ LCSCs. (B) Sphere formation assay of the effect of B4GALNT1 knockdown or overexpression on sphere formation ability. (C) Cell proliferation assay of the effect of B4GALNT1 knockdown or overexpression on HCC cell proliferation. (D) Transwell migration assay of the effect of B4GALNT1 knockdown or overexpression on HCC cell migration ability. (E) Transwell invasion assay of the effect of B4GALNT1 knockdown or

concentrations are shown in Table S3. After washing with PBS, cells were incubated with secondary antibodies and counterstained with DAPI (1 μg/ml). Pictures were taken under either a fluorescence or confocal microscope.

Immunoprecipitation and mass spectrometry analysis

HCC cells were homogenised in NP-40 lysis buffer (Beyotime Biotechnology, China). Equal amounts of protein extracts were incubated with primary antibodies overnight at 4 °C. Then, Dynabeads™ Protein G (Thermo Fisher Scientific) were added and the mixture was incubated at 4 °C overnight. After washing with PBS, the beads were eluted with 40 μl SDT lysis buffer, and the eluted protein complexes were detected by silver staining, mass spectrometry, and western blotting.

For mass spectrometry analysis, after reduction and alkylation treatment, the sample was enzymatically hydrolysed with trypsin (mass ratio 1:50) at 37 °C for 20 h, the hydrolysate was then desalted, freeze-dried, redissolved in 0.1% formic acid solution, and stored at –20 °C for use. A chromatographic column was equilibrated in 95% Liquid A (an aqueous solution of 0.1% formic acid) and the sample was then loaded into the Trap column by an automatic sampler. The mass charge ratio of polypeptides and polypeptide fragments was collected as follows: 20 fragments were collected after each full scan (MS2 scan). Mass spectrometry test raw files were retrieved from the corresponding database using Proteome Discoverer 1.4 software and then identified.

Bioinformatic analysis

StarBase V3.0 and GEPIA were used to analyse the expression of *B4GALNT1* and *ITGB1* in HCC and normal tissues. KMplotter was used to analyse the correlation between the expression of B4GALNT1 and ITGB1 and the clinical outcome of patients with HCC. For RNA-sequencing (RNA-seq) analysis, all reads were aligned to the human reference genome hg19 using Burrows–Wheeler Aligner (BWA). Aligned reads were converted to the Sequence Alignment/Map (SAM/BAM) format using SAMtools.

In vivo tumourigenicity assay

All animal procedures were performed in accordance with the Guide for the Care and Use of Laboratory Animals (National Institutes of Health publications Nos. 80–23, revised 1996) and were approved by the Institutional Animal Care and Use Committee of the Fifth Affiliated Hospital of Sun Yat-Sen University. Male BALB/c nude mice aged 4 to 5 weeks (GemPharmatech; n = 5/group) were subcutaneously injected in the flank with 5×10^6 HCC cells. Tumour growth was observed every 4 days, and the diameter of the tumour was measured with a vernier calliper. After 3 to 4 weeks, the mice were euthanised and the tumours were harvested and weighed.

Statistical analysis

Statistical analysis was performed using SPSS 24.0 (SPSS Inc., Chicago, IL, USA) and GraphPad Prism 5 (GraphPad Software Inc., San Diego, CA, USA) software. Data were presented as mean ± SD from at least three independent experiments. Kaplan-Meier survival curves were compared using the log-rank test. Comparisons between different groups were performed using the Student's two-tailed *t* test. Correlation analysis was achieved by Chi-square test and Pearson's correlation analysis. Differences were considered statistically significant at $p < 0.05$.

Results

B4GALNT1 is associated with poor outcomes for patients with HCC

We used a genome-wide CRISPR/Cas9 knockout system to systematically investigate the regulatory factors governing self-renewal in $CD24^+CD133^+$ LCSCs within PLC cell populations. Flow cytometry analysis substantiated that the downregulation of B4GALNT1, AP1S2, PUSL1, and TRIT1 profoundly curtailed the self-renewal potential of $CD24^+CD133^+$ LCSCs within PLC cell populations. Notably, the knockdown of B4GALNT1 resulted in the most substantial reduction in the proportion of $CD24^+CD133^+$ LCSCs (Fig. 1A), prompting us to select B4GALNT1 for in-depth exploration.

Turning our attention to the clinical relevance of B4GALNT1 in HCC, we initially scrutinised its expression in HCC cells and immortalised hepatocytes. qRT-PCR and western blot (WB) analyses unveiled a marked upregulation of B4GALNT1 in HCC cells (Fig. S1A,B). Subsequently, we assessed the expression of *B4GALNT1* in HCC tissues and normal liver tissues obtained from The Cancer Genome Atlas (TCGA). These investigations, facilitated by the ULCAN and Starbase v3.0 online algorithms, revealed a significant elevation of *B4GALNT1* expression in HCC tissues (Fig. 1B,C). Moreover, Kaplan-Meier survival analyses underscored that elevated *B4GALNT1* expression correlated with shorter overall- and recurrence-free survival durations compared with counterparts with lower *B4GALNT1* expression levels (Fig. 1D,E). Furthermore, IHC examination of 98 paired HCC tissues and ANTs solidified the observation of heightened B4GALNT1 expression in HCC tissues relative to ANTs (Fig. 1F). These results were further corroborated by statistical analysis, confirming the upregulation of B4GALNT1 in HCC tissues (Fig. 1G). Importantly, heightened B4GALNT1 expression was intricately linked with aggressive pathological attributes among patients with HCC, including increased tumour volume, diminished histological grade, advanced TNM stage, intensified capsular invasion, microvascular invasion, and satellite nodule formation (Table S4). Notably, Kaplan-Meier survival analyses reiterated that patients displaying heightened B4GALNT1 expression had reduced overall- and disease-free survival durations (Fig. 1H,I). Subsequent univariate and multivariate Cox regression analyses substantiated the status of B4GALNT1 as an independent prognostic determinant for patients with HCC (Table S5). Collectively, these findings firmly establish heightened B4GALNT1 expression as a predictor of an unfavourable prognosis for patients with HCC, solidifying its role as an independent prognostic factor.

overexpression on HCC cell invasion ability. (F) IF staining of E-cadherin and vimentin expression in HCC cells with B4GALNT1 knockdown or overexpression. (G) Effect of B4GALNT1 overexpression on HCC growth in a subcutaneous xenograft mouse model. The effect of B4GALNT1 overexpression on tumour volume and weight was also analysed. Data are mean±SEM for three technical replicates, analysed with the Student's two-tailed *t* test; *$p < 0.05$, **$p < 0.01$. Scale bars: 50 μm. B4GALNT1, β-1,4-*N*-acetyl-galactosaminyltransferase 1; HCC, hepatocellular carcinoma; IF, immunofluorescence; LCSC, liver cancer stem cell; shNC, negative control vector containing scrambled shRNA.

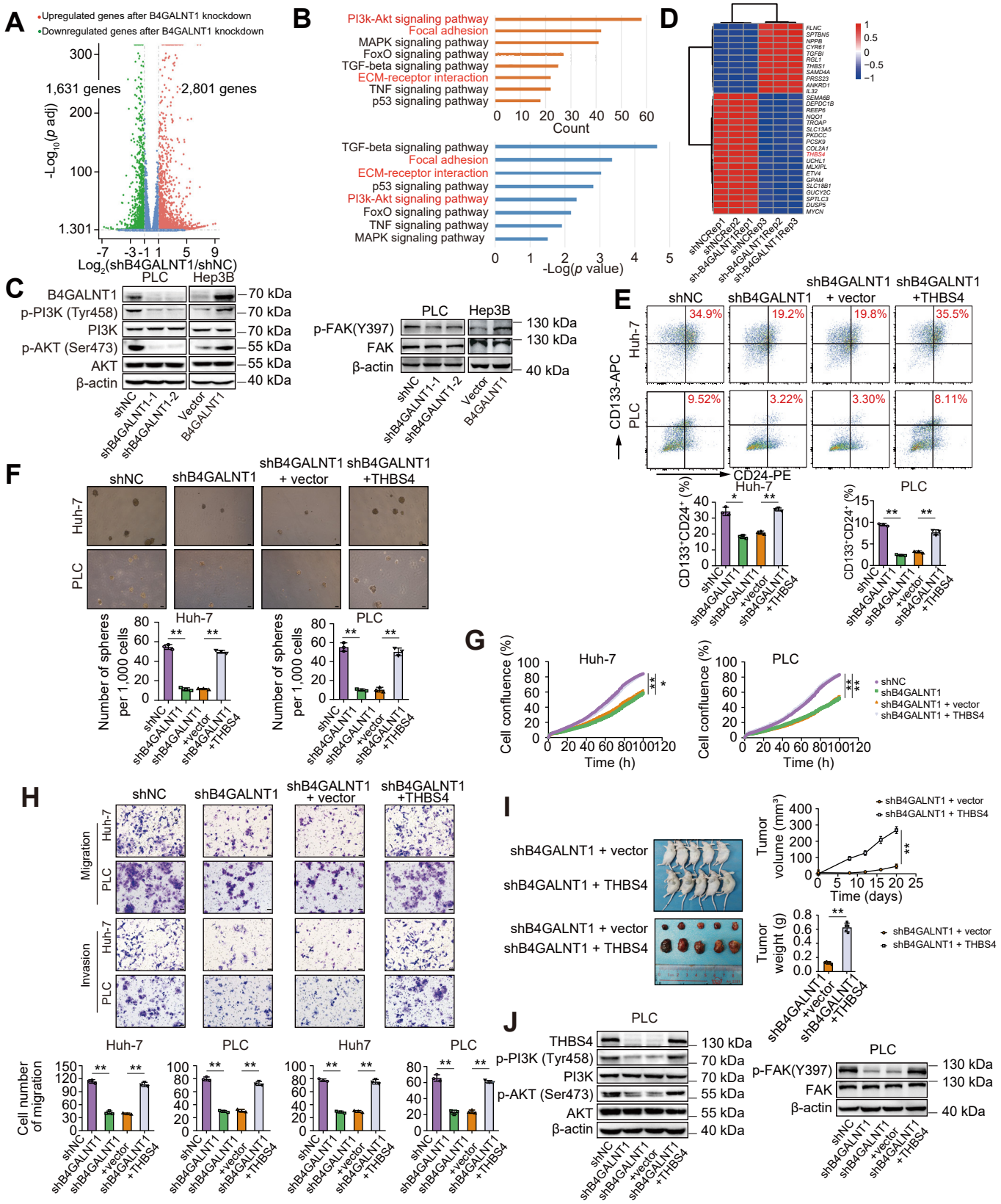

Fig. 3. B4GALNT1 promotes HCC stemness and progression by upregulating THBS4. (A) Volcano plot of relative gene expression in HCC cells transduced with shNC or shB4GALNT1. Red and green points indicate upregulated and downregulated target genes, respectively. (B) KEGG analysis of downregulated target genes. (C) Western blot of the phosphorylation levels of FAK, PI3K, and AKT after B4GALNT1 overexpression or knockdown. (D) Heatmap depicting normalised expression of the top ranked downregulated and upregulated genes in HCC cells with B4GALNT1 knockdown. (E) Flow cytometry analysis of the effect of THBS4

B4GALNT1 promotes HCC stemness, proliferation, migration, invasion, and growth

To elucidate the functional ramifications of B4GALNT1 in HCC initiation and progression, we harnessed shRNAs to suppress B4GALNT1 expression in Huh-7 and PLC cells, while also effecting B4GALNT1 overexpression in Huh-7 and Hep3B cells (Fig. S1C–F). Using flow cytometry and sphere formation assays, we investigated the involvement of B4GALNT1 in HCC stemness, revealing its propensity to significantly augment the population of $CD24^{+}CD133^{+}$ LCSCs and enhance sphere formation (Fig. 2A,B). Beyond its influence on HCC stemness, the role of B4GALNT1 extended to the facilitation of HCC cell proliferation, migration, and invasion, as corroborated by assays encompassing cell proliferation, migration (without Matrigel), invasion (with Matrigel) Transwell, and wound-healing assays (Fig. 2C–E and Fig. S2A,B). Given the established correlation between EMT and tumoural stemness and metastasis,[13] we investigated whether the impact of B4GALNT1 extended to EMT in HCC cells. Notably, immunofluorescence (IF) staining and WB assays validated the induction of EMT by B4GALNT1 (Fig. 2F and Fig. S2C,D). Complementary insight was gleaned from a xenograft tumour model, which highlighted the pivotal role of B4GALNT1 in regulating tumour growth. Notably, B4GALNT1 downregulation starkly attenuated tumour volume and weight, whereas B4GALNT1 overexpression prompted their augmentation (Figs 2G and 5E). Thus, these results unequivocally established the multifaceted contribution of B4GALNT1 to HCC stemness, proliferation, migration, invasion, EMT, and growth.

B4GALNT1 promotes HCC stemness and progression by regulating the integrin α2β1 ligand THBS4

The enzymatic function of B4GALNT1 is indispensable for GM2 and GD2 biosynthesis. Existing literature underscores the elevated presence of the gangliosides GM2/GD2 within breast cancer stem cells (BCSCs), where they significantly contribute to breast cancer stemness. Notably, GD2 serves as a surface marker of BCSCs,[14,15] further establishing its relevance. Interestingly, GD2 has also been harnessed as a target in chimeric antigen receptor-based immunotherapy.[14] The potential role of GD2 in mediating B4GALNT1-driven HCC stemness and progression has remained enigmatic. We found that B4GALNT1 knockdown exerted a suppressive effect on GD2 expression, whereas B4GALNT1 overexpression increased GD2 levels, as evidenced by IF staining (Fig. S3A). However, GD2 expression was not significantly disparate between HCC tissues and ANTs, as indicated by immunohistochemistry (IHC; Fig. S3B). This implies that the ability of B4GALNT1 to enhance HCC stemness and progression is not contingent on GD2 and, consequently, GD2 might not represent a viable target for HCC immunotherapy.

To unravel the underlying mechanism by which B4GALNT1 orchestrates HCC stemness and progression, we performed RNA-seq analysis to identify downstream targets governed by B4GALNT1 (Fig. 3A). Of particular interest was the integrin pathway, which actively participates in focal adhesion and ECM–receptor interactions. Ligand–integrin complexes operationalise FAK, thus relaying signals to the PI3K/AKT pathway.[7] KEGG analysis of differentially expressed genes (DEGs) triggered by B4GALNT1 knockdown accentuated significant enrichment within the PI3K/AKT pathway, focal adhesion, and ECM–receptor interactions (Fig. 3B). These pathways are intrinsically linked to the integrin/FAK/PI3K/AKT axis,[8] thereby positioning B4GALNT1 as a potential regulator of this axis. WB assays corroborated the role of B4GALNT1 in heightening the phosphorylation levels of PI3K (Tyr458), AKT (Ser473), and FAK (Ser397) (Fig. 3C and Fig. S3C), thereby confirming the ability of *B4GALNT1* to activate the integrin/FAK/PI3K/AKT pathway. Most notably, our analysis identified the gene encoding thrombospondin 4 (*THBS4*) as a leading candidate among the genes downregulated following B4GALNT1 knockdown (Fig. 3D). THBS4, acting as an integrin α2β1 ligand, interfaces with the α-subunit of integrin α2β1 (ITGA2) to potentiate the integrin pathway.[16,17] Existing research also underscores the role of THBS4 in fuelling HCC growth and metastasis by modulating the FAK/PI3K/AKT pathway.[18] To determine whether B4GALNT1 augments HCC stemness and progression via THBS4 regulation, we conducted THBS4 overexpression experiments in B4GALNT1-knockdown cells. Strikingly, THBS4 overexpression effectively rescued HCC stemness and restored cellular proliferation, migration, invasion, and growth in B4GALNT1-knockdown cells (Fig. 3E–I and Fig. S4A–C). Importantly, WB assays showcased the ability of THBS4 overexpression to counteract the inhibitory impact of B4GALNT1 knockdown on integrin/FAK/PI3K/AKT pathway activity, firmly establishing the role of B4GALNT1 in promoting the integrin/FAK/PI3K/AKT pathway via THBS4 (Fig. 3J and Fig. S4D). In summary, these findings unveil B4GALNT1 definitively as a facilitator of HCC stemness and progression through the elevation of THBS4 expression.

B4GALNT1 inhibits the ubiquitin-independent proteasomal degradation of ITGB1

To further determine the mechanism underlying the modulation of HCC stemness and progression by B4GALNT1, immunoprecipitation coupled with mass spectrometry (IP-MS) was used to scrutinise the B4GALNT1 interactome. This analysis identified the β-subunit of integrin α2β1 (ITGB1) as a prospective B4GALNT1-interacting protein within HCC cells (Fig. 4A). *ITGB1*, a recognised oncogene, is known for orchestrating HCC growth via its regulation of the PXN/YWHAZ/AKT[19] and PI3K/AKT pathways.[20] Furthermore, IF staining substantiated the colocalisation of B4GALNT1 and ITGB1 within HCC cells (Fig. 4B). Co-IP assays conclusively demonstrated the physical interaction between endogenous B4GALNT1 and ITGB1 (Fig. 4C,D), providing evidence that ITGB1 could represent a direct downstream target of B4GALNT1 within HCC cells.

Subsequent investigations aimed to ascertain whether B4GALNT1 exerts influence over ITGB1 expression. Through qRT-PCR and WB analyses, it was revealed that the influence of

overexpression on the percentage of $CD24^{+}CD133^{+}$ LCSCs in HCC cells with B4GALNT1 knockdown. (F) Sphere formation assay of the effect of THBS4 overexpression on sphere formation ability in HCC cells with B4GALNT1 knockdown. (G) Cell proliferation assay of the effect of THBS4 overexpression on cellular proliferation in HCC cells with B4GALNT1 knockdown. (H) Transwell migration and invasion assay of the effect of THBS4 overexpression on cellular migration and invasion ability in HCC with B4GALNT1 knockdown. (I) Tumour growth analysis in HCC cells transduced with either shB4GALNT1 alone or shB4GALNT1 and THBS4 together. (J) Western blot of the phosphorylation of FAK, PI3K, and AKT in HCC cells transduced with either shB4GALNT1 alone or shB4GALNT1 and THBS4 overexpression vectors. Data are mean ± SEM for three technical replicates, analysed with Student's two-tailed *t* test; $^{*}p$ <0.05, $^{**}p$ <0.01. Scale bars: 50 μm (H), 100 μm (F). B4GALNT1, β-1,4-*N*-acetyl-galactosaminyltransferase 1; HCC, hepatocellular carcinoma; LCSC, liver cancer stem cell; PLC, PLC/PRF/5 cell line; shNC, negative control vector containing scrambled shRNA; THBS4, thrombospondin 4.

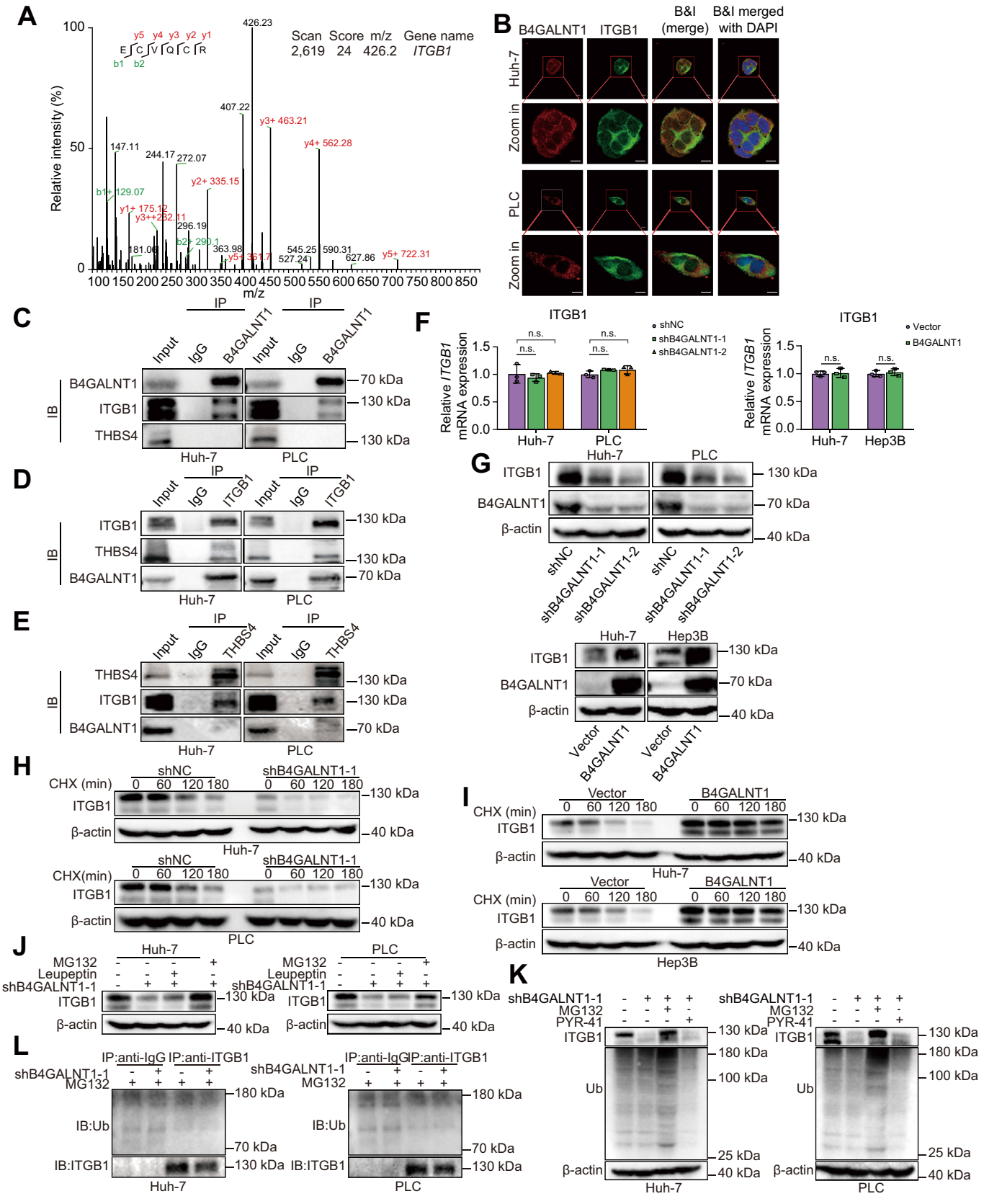

Fig. 4. B4GALNT1 interacts directly with ITGB1 to increase the protein stability of ITGB1. (A) A unique peptide of ITGB1 was identified in B4GALNT1 immunoprecipitation samples by analysing the mass-to-charge ratio of the samples. (B) IF staining assay of the colocalisation of B4GALNT1 and ITGB1. (C–E) Co-IP analysis of the interaction among endogenous B4GALNT1, THBS4, and ITGB1 in HCC cells. (F) qRT-PCR analysis of the effect of *B4GALNT1* knockdown or overexpression on ITGB1 mRNA level. (G–I) Western blot of the effect of B4GALNT1 knockdown or overexpression on (G) ITGB1 protein level and (H,I) ITGB1 stability

B4GALNT1 did not extend to the mRNA level of ITGB1; instead, it intricately regulated the protein level of ITGB1. This intriguing pattern suggested that B4GALNT1 presides over the stability of ITGB1 protein (Fig. 4F,G). This hypothesis was corroborated by experiments involving the use of cycloheximide (CHX), a protein synthesis inhibitor, in HCC cells transduced with either a negative control, a B4GALNT1 overexpression vector, or a B4GALNT1 knockdown vector. Remarkably, B4GALNT1 overexpression effectively counteracted ITGB1 protein degradation, as demonstrated by the results from the CHX treatment experiments (Fig. 4H–I and Fig. S5).

ITGB1 degradation follows the well-documented pathways of both lysosomal and proteasomal degradation.[20] Notably, our investigation showed that the diminished ITGB1 protein expression level resulting from B4GALNT1 knockdown could be completely restored through treatment with the proteasome inhibitor MG132. Conversely, the lysosome inhibitor leupeptin exhibited negligible impact on ITGB1 levels (Fig. 4J). Intriguingly, integrins have previously been linked with ubiquitination-mediated sorting and degradation.[20] We used an ubiquitination assay to determine whether B4GALNT1 prevents ITGB1 degradation via a ubiquitin-dependent mechanism. The findings revealed that MG-132 treatment increased total ubiquitination levels while concurrently inhibiting ITGB1 degradation in B4GALNT1-knockdown HCC cells. However, the ubiquitin-activating enzyme inhibitor PYR-41 reduced total ubiquitination levels without significantly impeding the degradation of ITGB1 catalysed by B4GALNT1 knockdown (Fig. 4K). Additionally, ITGB1 could not be ubiquitinated even in the presence of MG132. (Fig. 4L), highlighting the propensity of B4GALNT1 to curtail ITGB1 degradation via a ubiquitination-independent route. Thus, these comprehensive results collectively underscore the ability of B4GALNT1 to form an interaction with ITGB1, thereby inhibiting the ubiquitin-independent proteasomal degradation of ITGB1.

Furthermore, an intriguing observation emerged of the interaction of ITGB1 with THBS4 within HCC cells (Fig. 4D,E), corroborating previous findings[18] and substantiating the synergy between THBS4 and ITGA2 in activating the integrin α2β1/FAK/PI3K/AKT pathway.

B4GALNT1 promotes HCC stemness and progression via ITGB1

A subsequent inquiry aimed to elucidate the mechanism underlying the promotion of HCC stemness and progression through ITGB1 regulation by B4GALNT1. Remarkably, ITGB1 overexpression effectively nullified the inhibitory impact of B4GALNT1 knockdown on HCC stemness and crucial facets of cellular behaviour, including proliferation, migration, invasion, and growth. The orchestration of HCC stemness and progression by B4GALNT1 crucially hinged on its regulation of ITGB1 (Fig. 5A–E and Fig. S6A,B). This effect was further underscored by WB assays, which showed the ability of ITGB1 to restore integrin/FAK/PI3K/AKT pathway activity within B4GALNT1-knockdown HCC cells (Fig. 5F).

Interestingly, although a direct interaction between B4GALNT1 and THBS4 within HCC cells was not established (Fig. 4C,E), ITGB1 emerged as a key player in fostering THBS4 expression within HCC (Fig. 5F and Fig. S6C). These nuanced insights collectively support the role of B4GALNT1 in driving integrin/FAK/PI3K/AKT pathway activity and THBS4 expression through its regulation of ITGB1.

Furthermore, although the link between B4GALNT1 and ITGB1 stability has been well demonstrated, further exploration of this relationship within samples from patients with HCC has been lacking. IHC assays of tissue specimens revealed a significant elevation of ITGB1 in HCC tissues compared with their corresponding ANTs (Fig. 6A,B). The clinical implications of this were unveiled through Kaplan-Meier survival curves, which starkly showcased shorter overall- and disease-free survival durations among patients with elevated ITGB1 expression compared with their low-expression counterparts (Fig. 6C,D). A positive correlation between B4GALNT1 and ITGB1 expression was unveiled through correlation analysis ($r = 0.6717$, $p < 0.0001$) (Fig. 6E,F). Notably, the correlation analysis was also extended to the relationship between B4GALNT1 and THBS4 expression through additional IHC analysis (Fig. S7A). These data underscored a significant positive correlation between B4GALNT1 and THBS4 expression in HCC tissues ($r = 0.5079$, $p < 0.01$) (Fig. S7B,C). In summary, a correlation emerges, effectively linking B4GALNT1, THBS4, and ITGB1 expression levels within the context of HCC.

Ophiopogonin D effectively inhibits HCC stemness and progression

OP-D, a steroidal glycoside derived from the Chinese herb Radix *Ophiopogon japonicus*, has garnered attention for its potential as an anticancer agent. This compound has demonstrated efficacy against various malignancies, including breast cancer and lung carcinoma.[21,22] Notably, previous studies revealed the ability of OP-D to curtail TGF-β1-mediated metastasis in triple-negative breast cancer cells by exerting influence over the ITGB1/FAK/Src/AKT/β-catenin/MMP-9 signalling axis,[23] effectively positioning OP-D as an inhibitor of ITGB1-associated pathways. Determination of the 50% inhibitory concentration (IC_{50}) of OP-D over a 48-h interval in HCC cells (Fig. S8) informed subsequent studies in which a low-toxic concentration of OP-D (10 μM) was used. Findings demonstrating that OP-D intervention effectively stifled HCC stemness, migration, invasion, growth, and integrin/FAK/PI3K/AKT pathway activity within B4GALNT1-overexpressing cells (Fig. S9A–F).

Furthermore, systematic exploration of the potential therapeutic utility of OP-D within HCC showed that OP-D treatment yielded profound reductions in HCC stemness, proliferation, migration, invasion, and growth (Fig. 7A–E). Additional insights revealed that OP-D treatment effectively dampened the expression of ITGB1 and THBS4, along with suppressing integrin/FAK/PI3K/AKT pathway activity. Strikingly, whereas OP-D intervention effectively modulated ITGB1 and THBS4 expression, B4GALNT1 expression remained largely unaltered (Fig. 7F). These

in HCC cells incubated with CHX (5 μg/ml) at the indicated time points. (J) Western blot of the effect of MG132 (10 μM, 6 h) and leupeptin (10 μM, 24 h) on ITGB1 expression in HCC cells transduced with shB4GALNT1 or shNC. (K) Western blot of the effect of MG132 and PYR-41 (20 μM, 24 h) on the expression of ITGB1 and total Ub in HCC cells transduced with shB4GALNT1 or shNC. (L) Co-IP analysis of the level of ITGB1 ubiquitination in HCC cells transduced with shB4GALNT1 or shNC in the presence of MG132. Data are mean ± SEM for three technical replicates, analysed with Student's two-tailed *t* test; **p* <0.05, ***p* <0.01. Scale bars: 20 μm. B4GALNT1, β-1,4-*N*-acetyl-galactosaminyltransferase 1; CHX, cycloheximide; Co-IP, co-immunoprecipitation; HCC, hepatocellular carcinoma; IF, immunofluorescence; ITGB1, integrin β1; PLC, PLC/PRF/5 cell line; shNC, short hairpin negative control; Ub, ubiquitin.

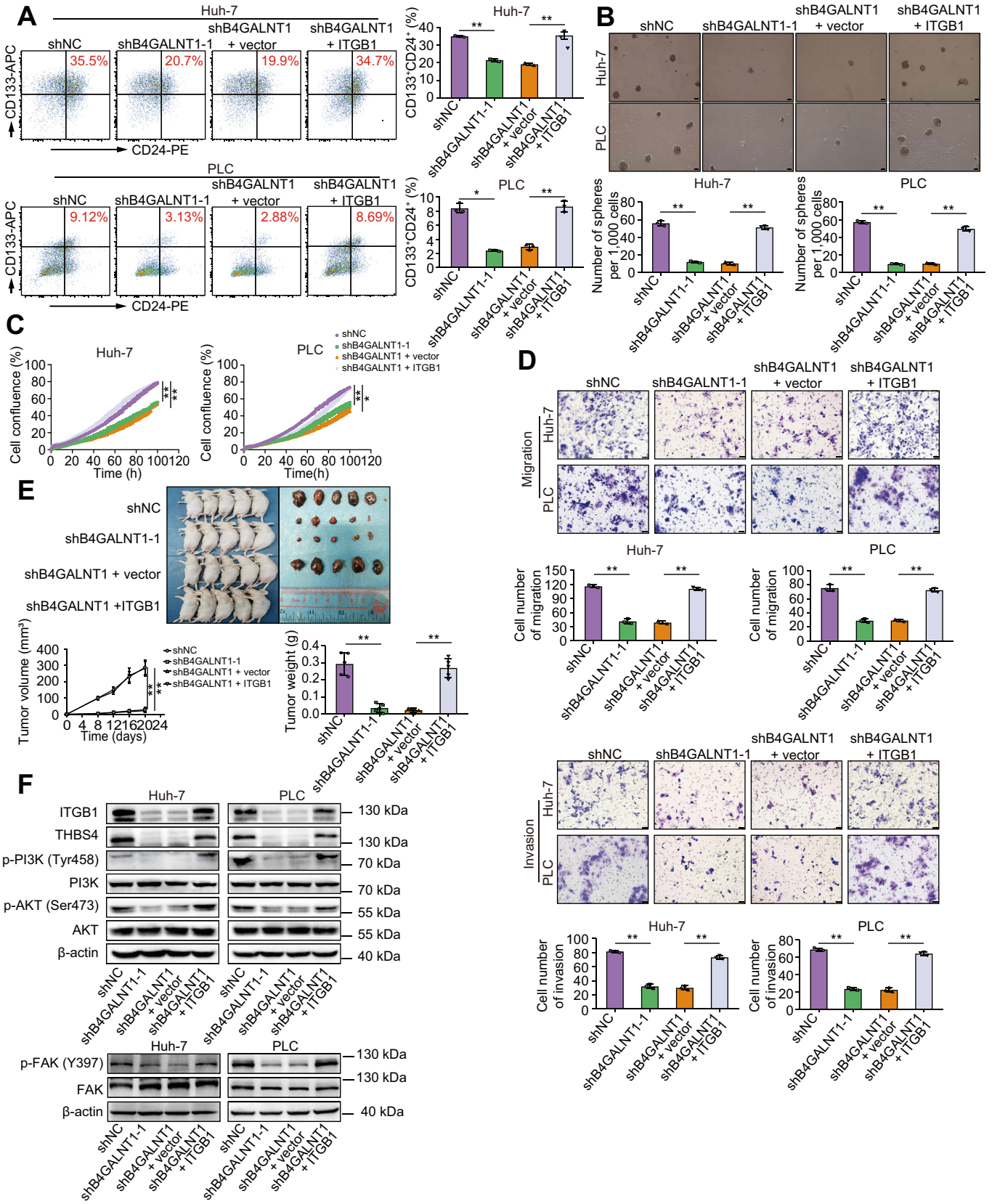

Fig. 5. ITGB1 overexpression restores the inhibitory effect of B4GALNT1 knockdown on HCC stemness, proliferation, migration, invasion, and growth. (A) Flow cytometry analysis of the effect of ITGB1 overexpression on the percentage of $CD24^{+}CD133^{+}$ LCSCs in HCC cells with B4GALNT1 knockdown. (B) Sphere formation assay of the effect of ITGB1 overexpression on sphere formation ability in HCC cells with B4GALNT1 knockdown. (C) Cell proliferation assay of the effect of ITGB1 overexpression on cellular proliferation in HCC cells with B4GALNT1 knockdown. (D) Transwell migration and invasion assay of the effect of ITGB1

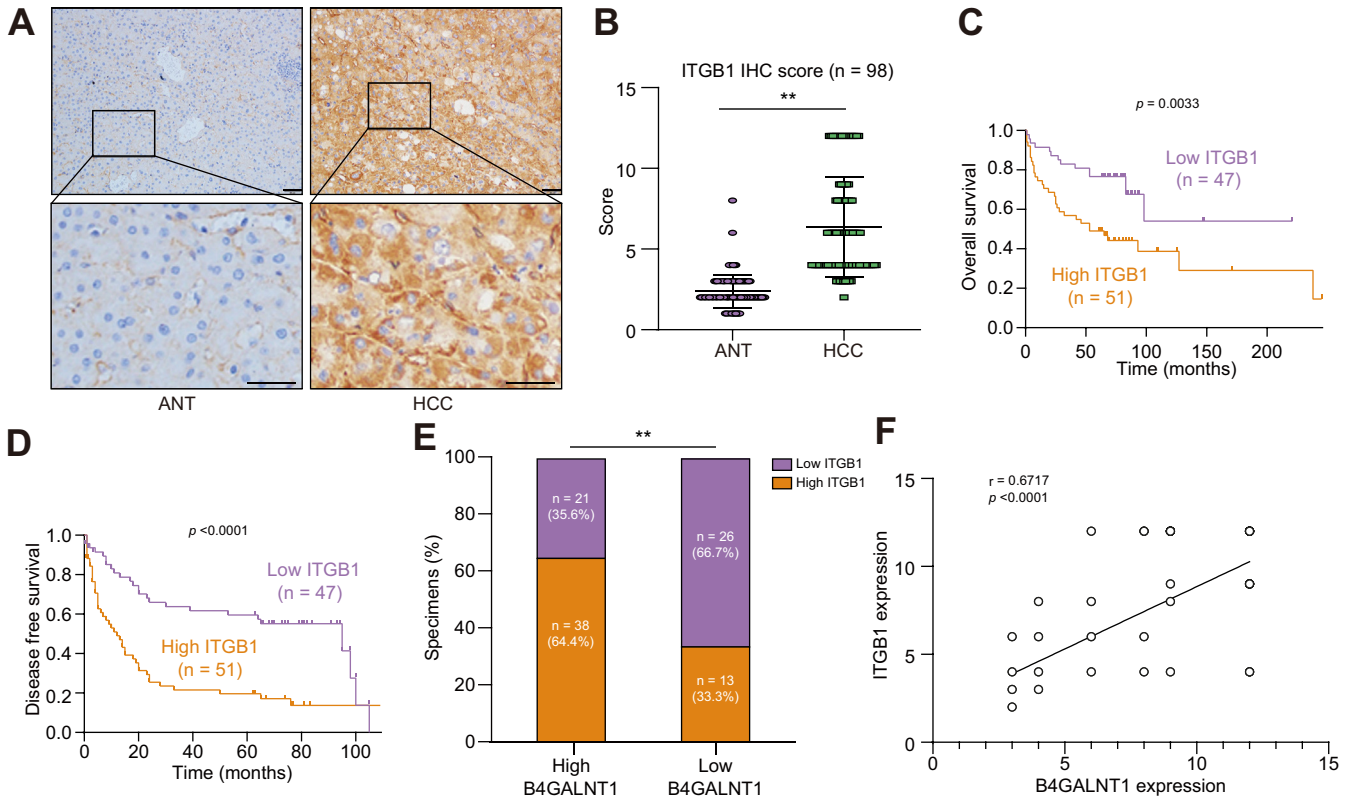

Fig. 6. ITGB1 is associated with worse clinical outcomes for patients with HCC and positively correlates with B4GALNT1 expression. (A) Representative image of IHC staining of ITGB1 in HCC tissues and ANTs. (B) Differential ITGB1 expression level in HCC tissues and paired normal liver tissues were evaluated by Wilcoxon signed-rank test. Kaplan-Meier curves for overall survival (C) and recurrence-free survival (D) of 98 patients with HCC with low *vs.* high ITGB1 expression. Kaplan-Meier survival curves were compared using the log-rank test. (E) Correlation between B4GALNT1 and ITGB1 proteins in 98 patients with HCC evaluated by Chi-square test; $^{**}p$ <0.01. (F) Pearson's correlation analysis between B4GALNT1 and ITGB1 proteins in 98 patients with HCC. Scale bars: 50 μm. ANT, adjacent normal liver tissue; B4GALNT1, β-1,4-*N*-acetyl-galactosaminyltransferase 1; HCC, hepatocellular carcinoma; IHC, immunohistochemistry; ITGB1, integrin β1; LCSC, liver cancer stem cell.

compelling findings lay the foundation for considering OP-D as a potential therapeutic candidate for the treatment of HCC.

Discussion

This study highlights a pivotal role for B4GALNT1 in supporting HCC progression by orchestrating the expression of THBS4 and enhancing the stability of ITGB1 proteins, thereby fortifying integrin α2β1–ligand complexes. Additionally, our results reveal the therapeutic potential of the steroidal glycoside OP-D as an effective inhibitor of HCC stemness and progression and underscore the significance of the B4GALNT1/integrin α2β1/FAK/PI3K/AKT axis in propelling HCC development.

The aberrant activation of integrins has profound implications for tumour processes, such as migration, invasion, metastasis, survival, and resistance to therapies.[24,25] THBS4, an extracellular matricellular protein rich in calcium-binding domains, is an important ligand of integrin α2β1, participating in a spectrum of biological phenomena, including neural development, cardiomyopathy, and tumour progression.[26] For instance, the THBS4/ITGA2 axis has been associated with promoting angiogenesis in gastric cancer.[16] ITGB1, constituting the β-subunit of integrin α2β1, has been acknowledged for its role in governing HCC proliferation, invasion, and metastasis. Yet, the precise contributions of THBS4 and ITGB1 to HCC stemness have remained largely uncharted. Our investigation unveiled that B4GALNT1 not only fosters the expression of THBS4, but also engages in direct interactions with ITGB1. This interaction augments the stability of ITGB1 protein, thus forestalling its degradation through the ubiquitination-independent proteasomal pathway. Moreover, the interplay between ITGB1 andTHBS4 facilitates the recruitment of THBS4 to ITGA2, further consolidating this intricate network. These findings offer insights into the role of B4GALNT1 in increasing the stability of THBS4–integrin α2β1 complexes and perpetuating integrin α2β1/FAK/PI3K/AKT pathway activity, highlighting B4GALNT1 as a pivotal actor in activation of the integrin α2β1 pathway (Fig. 7G).

overexpression on cellular migration and invasion ability in HCC with B4GALNT1 knockdown. (E) Tumourigenicity analysis in HCC cells transduced with either shB4GALNT1 alone or shB4GALNT1 and ITGB1 together. (F) Western blot of the levels of THBS4, and phosphorylation of FAK, PI3K, and AKT in HCC cells transduced with either shB4GALNT1 alone or shB4GALNT1 and ITGB1 overexpression vector together. Data are mean ± SEM for three technical replicates, analysed with Student's two-tailed *t* test; $^{*}p$ <0.05, $^{**}p$ <0.01. Scale bars: 50 μm (D), 100 μm (B). B4GALNT1, β-1,4-*N*-acetyl-galactosaminyltransferase 1; HCC, hepatocellular carcinoma; ITGB1, integrin β1; PLC, PLC/PRF/5 cell line; shNC, short hairpin negative control; Ub, ubiquitin.

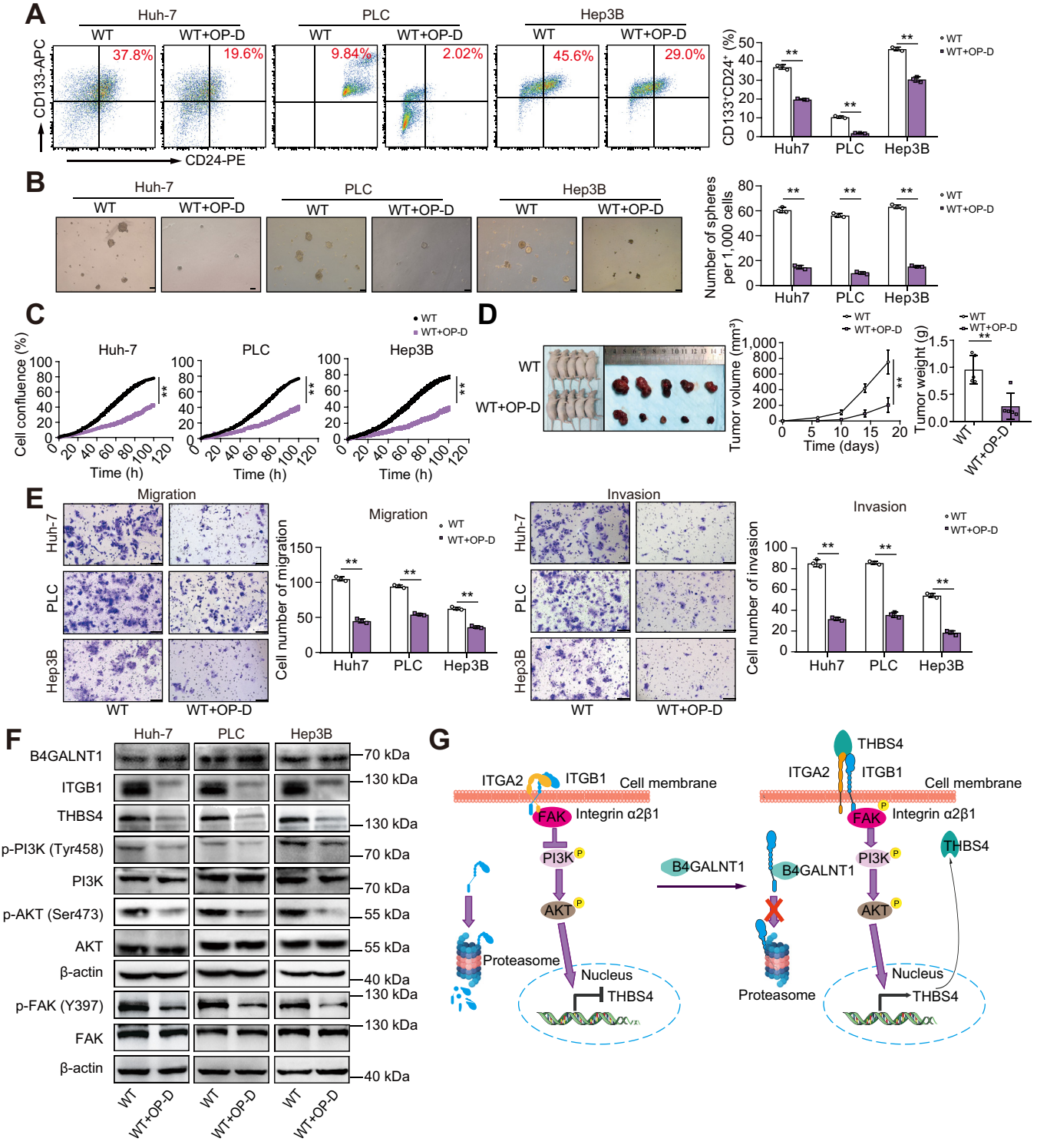

Fig. 7. OP-D inhibits HCC stemness and progression by inhibiting ITGB1 and THBS4. (A) Flow cytometry analysis of the effect of OP-D on the percentage of $CD24^{+}CD133^{+}$ LCSCs in HCC cells. (B) Sphere formation assay of the effect of OP-D on sphere formation ability in HCC cells. (C) Cell proliferation assay of the effect of OP-D on cellular proliferation in HCC cells. (D) Tumourigenicity analysis in HCC cells treated with OP-D. (E) Transwell migration and invasion assay of the effect of OP-D on the cellular migration and invasion ability of HCC cells. (F) Western blot of OP-D treatment on the levels of ITGB1, THBS4, and phosphorylation of FAK, PI3K, and AKT in HCC cells. (G) Working model schematic. Data are mean ± SEM for three technical replicates, analysed with Student's two-tailed *t* test; $^{*}p$ <0.05, $^{**}p$ <0.01. Scale bars: 50 μm (E), 100 μm (B). HCC, hepatocellular carcinoma; ITGA2, integrin α2; ITGB1, integrin β1; LCSC, LCSC, liver cancer stem cell; OP-D, ophiopogonin D; PLC, PLC/PRF/5 cell line; THBS4, thrombospondin 4; WT, wild type.

The central role of integrin α2β1 in diverse facets of cancer biology, including proliferation, invasion, angiogenesis, metastasis, and chemoresistance, has been well documented.[27] The current study adds to this understanding by revealing the impact of integrin α2β1 on HCC stemness, highlighting targeting integrin α2β1 as a potential HCC treatment. Notably, the sulfonamide derivative E8720 curtails expression of the THSB4 receptor ITGA2, suggesting it as a candidate HCC therapy.[28]

An area requiring further exploration is the mechanism underpinning the regulation of THBS4 by B4GALNT1. While our findings underscore the role of ITGB1 in promoting THBS4 expression (Fig. S6C), the PI3K inhibitor LY294002 was observed to reverse heightened THBS4 expression in B4GALNT1-overexpressing cells (Fig. S10A,B). Hence, we suggest THBS4 as a downstream target of the FAK/PI3K/AKT pathway. The orchestrated interplay between B4GALNT1, ITGB1, and the FAK/PI3K/AKT pathway could culminate in a positive feedback loop driving THBS4 expression, a hypothesis that warrants further validation.

In light of these findings, targeting the B4GALNT1/integrin α2β1/FAK/PI3K/AKT axis emerges as a promising avenue for the development of innovative HCC therapeutic strategies. Thus, this study also explored the therapeutic potential of OP-D against HCC stemness and progression. The efficacy of OP-D in inhibiting HCC stemness and progression, as well as its capacity to counteract the impact of B4GALNT1 overexpression on these processes by targeting the B4GALNT1/integrin α2β1/FAK/PI3K/AKT axis, reinforces the prospect of OP-D as a potent therapeutic agent for HCC treatment. The clinical utility of OP-D could be further corroborated through *in vivo* HCC models and HCC organoids.

In conclusion, our study highlights the multifaceted role of B4GALNT1 in advancing HCC stemness and progression through its influence on ITGB1 stability and promotion of THBS4 expression, supporting integrin α2β1–ligand complex formation. Additionally, OP-D emerges as a promising contender for HCC therapy, bearing the potential to confer a considerable therapeutic impact for patients.

Abbreviations

ANT, adjacent normal liver tissue; B4GALNT1, β-1,4-*N*-acetyl-galactosaminyltransferase 1; BCSC, breast cancer stem cell; BSA, bovine serum albumin; BWA, Burrows–Wheeler Aligner; CHX, cycloheximide; DAB, 3,3′-diaminobenzidine; DEG, differentially expressed genes; ECM, extracellular matrix; EMT, epithelial–mesenchymal transition; HCC, hepatocellular carcinoma; IHC, immunohistochemistry; IF, immunofluorescence; IP-MS, immunoprecipitation coupled with mass spectrometry; ITGA2, integrin α2; ITGB1, integrin β1; LCSC, liver cancer stem cell; OP-D, Ophiopogonin D; PLC, PLC/PRF/5; RNA-seq, RNA-sequencing; qRT-PCR, quantitative real-time PCR; SAM/BAM, Sequence Alignment/Map; shRNA, short hairpin RNA; TCGA, The Cancer Genome Atlas; THBS4, thrombospondin 4; WB, western blot.

Financial support

This work is supported by the National Natural Science Foundation of China (81870411 and 82172241), Natural Science Foundation of Guangdong Province, China (2019A1515010138), Science and Technology Planning Project of Guangdong Province China (2019A030317017), and The Innovation Research Team for Basic and Clinical Studies on Chronic Liver Diseases of 2018 High-Level Health Teams of Zhuhai.

Conflicts of interest

The authors declare no conflicts of interest that pertain to this work.

Please refer to the accompanying ICMJE disclosure forms for further details.

Authors' contributions

Performed the experiments: YT, ZJX, FYX, JY, JXC, YCC, CHQ, RYL. Contributed to bioinformatics analysis: YCC, ZJX, HHH. Collected human tissues and clinical data:YT, ZJX, FYX, JY, JZH. Completed follow-up: YT, ZJX, FYX, JY, CHQ. Contributed to the animal experiments: YT, JIX, FYX, CHQ. Analyzed the data: YT, FX. Wrote the manuscript: YT, FX. Conceived and designed the experiments: FX, HS. Read and approved the manuscript: all authors.

Data availability statement

The data supporting the findings of this study are available from the corresponding author upon reasonable request. All the sequences have been deposited in the NCBI Gene Expression Omnibus (GEO) repository (PRJNA870716).

Acknowledgements

We thank the Research Core Facility of Guangdong Provincial Engineering Research Center of Molecular Imaging.

Supplementary data

Supplementary data to this article can be found online at https://doi.org/10.1016/j.jhepr.2023.100903.

References

Author names in bold designate shared co-first authorship

[1] Sung H, Ferlay J, Siegel RL, Laversanne M, Soerjomataram I, Jemal A, et al. Global Cancer Statistics 2020: GLOBOCAN Estimates of Incidence and Mortality Worldwide for 36 Cancers in 185 Countries. CA Cancer J Clin 2021;71:209–249.

[2] McGlynn KA, Petrick JL, El-Serag HB. Epidemiology of hepatocellular carcinoma. Hepatology 2021;73(Suppl 1):4–13.

[3] Llovet JM, Kelley RK, Villanueva A, Singal AG, Pikarsky E, Roayaie S, et al. Hepatocellular carcinoma. Nat Rev Dis Primers 2021;7:6.

[4] Yoshida H, Koodie L, Jacobsen K, Hanzawa K, Miyamoto Y, Yamamoto M. B4GALNT1 induces angiogenesis, anchorage independence growth and motility, and promotes tumorigenesis in melanoma by induction of ganglioside GM2/GD2. Sci Rep 2020;10:1199.

[5] Jiang T, Wu H, Lin M, Yin J, Tan L, Ruan Y, et al. B4GALNT1 promotes progression and metastasis in lung adenocarcinoma through JNK/c-Jun/Slug pathway. Carcinogenesis 2021;42:621–630.

[6] **Yang H**, **Li W**, Lv Y, Fan Q, Mao X, Long T, et al. Exploring the mechanism of clear cell renal cell carcinoma metastasis and key genes based on multi-tool joint analysis. Gene 2019;720:144103.

[7] Bouvard D, Pouwels J, De Franceschi N, Ivaska J. Integrin inactivators: balancing cellular functions in vitro and in vivo. Nat Rev Mol Cell Biol 2013;14:430–442.

[8] Kechagia JZ, Ivaska J, Roca-Cusachs P. Integrins as biomechanical sensors of the microenvironment. Nat Rev Mol Cell Biol 2019;20:457–473.

[9] Yang C, Zeisberg M, Lively JC, Nyberg P, Afdhal N, Kalluri R. Integrin alpha1beta1 and alpha2beta1 are the key regulators of hepatocarcinoma cell invasion across the fibrotic matrix microenvironment. Cancer Res 2003;63:8312–8317.

[10] Wong KF, Liu AM, Hong W, Xu Z, Luk JM. Integrin alpha2beta1 inhibits MST1 kinase phosphorylation and activates Yes-associated protein oncogenic signaling in hepatocellular carcinoma. Oncotarget 2016;7:77683–77695.

[11] **Yan F**, **Li J**, **Milosevic J**, Petroni R, Liu S, Shi Z, et al. KAT6A and ENL form an epigenetic transcriptional control module to drive critical leukemogenic gene-expression programs. Cancer Discov 2022;12:792–811.

[12] Lee TK, Guan XY, Ma S. Cancer stem cells in hepatocellular carcinoma – from origin to clinical implications. Nat Rev Gastroenterol Hepatol 2022;19:26–44.

[13] Dongre A, Weinberg RA. New insights into the mechanisms of epithelial-mesenchymal transition and implications for cancer. Nat Rev Mol Cell Biol 2019;20:69–84.

[14] **Majzner RG**, **Ramakrishna S**, Yeom KW, Patel S, Chinnasamy H, Schultz LM, et al. GD2-CAR T cell therapy for H3K27M-mutated diffuse midline gliomas. Nature 2022;603:934–941.
[15] Battula VL, Shi Y, Evans KW, Wang RY, Spaeth EL, Jacamo RO, et al. Ganglioside GD2 identifies breast cancer stem cells and promotes tumorigenesis. J Clin Invest 2012;122:2066–2078.
[16] He L, Wang W, Shi H, Jiang C, Yao H, Zhang Y, et al. THBS4/integrin alpha2 axis mediates BM-MSCs to promote angiogenesis in gastric cancer associated with chronic Helicobacter pylori infection. Aging (Albany NY) 2021;13:19375–19396.
[17] Stenina-Adognravi O, Plow EF. Thrombospondin-4 in tissue remodeling. Matrix Biol 2019;75–76:300–313.
[18] Guo D, Zhang D, Ren M, Lu G, Zhang X, He S, et al. THBS4 promotes HCC progression by regulating ITGB1 via FAK/PI3K/AKT pathway. FASEB J 2020;34:10668–10681.
[19] Xie J, Guo T, Zhong Z, Wang N, Liang Y, Zeng W, et al. ITGB1 drives hepatocellular carcinoma progression by modulating cell cycle process through PXN/YWHAZ/AKT pathways. Front Cell Dev Biol 2021;9:711149.
[20] **Shi L**, **Liu B**, Shen DD, Yan P, Zhang Y, Tian Y, et al. A tumor-suppressive circular RNA mediates uncanonical integrin degradation by the proteasome in liver cancer. Sci Adv 2021;7.
[21] Lee JH, Kim C, Lee SG, Sethi G, Ahn KS. Ophiopogonin D, a steroidal glycoside abrogates STAT3 signaling cascade and exhibits anti-cancer activity by causing GSH/GSSG imbalance in lung carcinoma. Cancers (Basel) 2018;10.
[22] Zang QQ, Zhang L, Gao N, Huang C. Ophiopogonin D inhibits cell proliferation, causes cell cycle arrest at G2/M, and induces apoptosis in human breast carcinoma MCF-7 cells. J Integr Med 2016;14:51–59.
[23] Zhu X, Wang K, Chen Y. Ophiopogonin D suppresses TGF-beta1-mediated metastatic behavior of MDA-MB-231 breast carcinoma cells via regulating ITGB1/FAK/Src/AKT/beta-catenin/MMP-9 signaling axis. Toxicol In Vitro 2020;69:104973.
[24] Hamidi H, Ivaska J. Every step of the way: integrins in cancer progression and metastasis. Nat Rev Cancer 2018;18:533–548.
[25] Newham P, Humphries MJ. Integrin adhesion receptors: structure, function and implications for biomedicine. Mol Med Today 1996;2:304–313.
[26] Vanhoutte D, Schips TG, Kwong JQ, Davis J, Tjondrokoesoemo A, Brody MJ, et al. Thrombospondin expression in myofibers stabilizes muscle membranes. Elife 2016;5.
[27] Naci D, Vuori K, Aoudjit F. Alpha2beta1 integrin in cancer development and chemoresistance. Semin Cancer Biol 2015;35:145–153.
[28] **Mita M**, **Kelly KR**, Mita A, Ricart AD, Romero O, Tolcher A, et al. Phase I study of E7820, an oral inhibitor of integrin alpha-2 expression with antiangiogenic properties, in patients with advanced malignancies. Clin Cancer Res 2011;17:193–200.